

S100A1 deficiency results in prolonged ventricular repolarization in response to sympathetic activation

G. E. Ackermann¹, A. A. Domenighetti², A. Deten³, I. Bonath¹, I. Marenholz⁴, T. Pedrazzini⁵, P. Erne⁶ and C. W. Heizmann¹

¹ Division of Clinical Chemistry and Biochemistry, Department of Pediatrics, University of Zürich, Steinwiesstrasse 75, 8032 Zürich, Switzerland

² Department of Medicine, The University of California in San Diego, La Jolla, USA

³ Institute of Veterinary Physiology, University of Zürich, Zürich, Switzerland

⁴ Max-Delbrück-Centrum for Molecular Medicine, Berlin, Germany

⁵ Department of Medicine, University of Lausanne Medical School, CHUV, Lausanne, Switzerland

⁶ Cantonal Hospital of Lucerne, Department of Cardiology, Lucerne, Switzerland

Abstract. S100A1 is a Ca²⁺-binding protein and predominantly expressed in the heart. We have generated a mouse line of S100A1 deficiency by gene trap mutagenesis to investigate the impact of S100A1 ablation on heart function. Electrocardiogram recordings revealed that after β -adrenergic stimulation S100A1-deficient mice had prolonged QT, QTc and ST intervals and intraventricular conduction disturbances reminiscent of 2 : 1 bundle branch block. In order to identify genes affected by the loss of S100A1, we profiled the mutant and wild type cardiac transcriptomes by gene array analysis. The expression of several genes functioning to the electrical activity of the heart were found to be significantly altered. Although the default prediction would be that mRNA and protein levels are highly correlated, comprehensive immunoblot analyses of salient up- or down-regulated candidate genes of any cellular network revealed no significant changes on protein level. Taken together, we found that S100A1 deficiency results in cardiac repolarization delay and alternating ventricular conduction defects in response to sympathetic activation accompanied by a significantly different transcriptional regulation.

Key words: S100A1 — Genetically altered mice — Heart — QT and ST intervals — Transcriptome profiling

Introduction

S100A1 is a member of the Ca²⁺-binding S100 protein family and involved in Ca²⁺-signalling (reviewed in Carafoli 2003; Donato 2003; Marenholz et al. 2004; Heizmann et al. 2007; Schaub and Heizmann 2008). S100A1 was demonstrated to interact with at least 24 different proteins in a Ca²⁺-dependent and -independent manner (reviewed in Santamaria-Kisiel et al. 2006). These include the sarcoplasmic reticulum Ca²⁺-ATPase 2a (SERCA2a), phospholamban (PLB) and the ryanodine receptor 2 (RyR2) (Kiewitz et al. 2003; Most et al. 2003). S100A1 is most prominently expressed in the heart, and present in cardiac and skeletal myocytes, astrocytes, neurons,

mammary cells, the kidney, liver, testes and adrenal gland (Kiewitz et al. 2000; Du et al. 2002; Zimmer et al. 2003, 2005; Ackermann et al. 2006).

The role of S100A1 was deduced *in vivo* by using a mouse model carrying a targeted deletion of the S100A1 protein-coding sequence (Du et al. 2002). Mutant as well as heterozygous mice failed to augment left ventricular systolic pressure, contraction and relaxation rates in response to β -adrenergic stimulation, whereas at rest cardiac function was normal. After myocardial infarction, S100A1^{-/-} mice showed more severely impaired contractility, relaxation and fractional shortening when compared to equally treated wild type (WT) mice (Most et al. 2006). In contrast, transgenic overexpression of S100A1 in the murine myocardium resulted in superior cardiac performance at rest and in response to β -adrenergic stimulation as reflected by augmented left ventricular systolic ejection pressure and enhanced contractility and relaxation rates (Most et al. 2003). In addition, both, transgenic overexpression as well as intracoronary viral

Correspondence to: Claus W. Heizmann, Division of Clinical Chemistry and Biochemistry, Department of Pediatrics, University of Zürich, Steinwiesstrasse 75, 8032 Zürich, Switzerland
E-mail: claus.heizmann@kispi.uzh.ch

S100A1 gene delivery were shown to be beneficial in preserving left ventricular function in infarcted rodents, proposing S100A1 as a candidate for gene therapy of potential clinical utility (Most et al. 2004, 2006; Pleger et al. 2007).

Here we report on the role of S100A1 in the electrical activity of the heart by using S100A1 knock out (S100A1KO) mice that were generated by gene trap mutagenesis (Ackermann et al. 2006). We discovered that, in response to sympathetic activation, loss of S100A1 resulted in prolonged ventricular repolarization and intraventricular conduction disturbances simulating 2 : 1 bundle branch block. Transcriptional profiling of the mutant heart revealed that several genes involved in controlling ion fluxes were differently regulated. Protein levels of salient up- and down-regulated genes were, however, unaffected, suggesting that transcription and protein synthesis are not necessarily coupled for the function and compensatory responsiveness of the S100A1-deficient heart.

Materials and Methods

Genetically modified mice

The generation, genetic characterization and breeding of S100A1-deficient mice were described previously (Ackermann et al. 2006). If not otherwise stated, mice backcrossed to C57BL/6J inbred mice for at least 10 generations were used for experiments. Mice were bred and maintained in an approved animal facility (Biologisches Zentrallabor, University of Zürich), and had access to food and water ad libitum. All animal procedures were performed in accordance with the Swiss animal protection law and the cantonal veterinary departments. To check for potential sex-specific differences, approximately equal numbers of males and females of each genotype (S100A1KO, WT) were used.

Heart-body weight indices, examination for fibrosis and cell size determination

The heart-body weight indices of S100A1KO and WT littermate mice were determined by calculating the ratio of the blotted heart weight and the body weight (mg/g).

For histology, freshly excised hearts were incubated in 30% sucrose in PBS for 2 h at 4°C, embedded in O.C.T. compound (Tissue-Tek, Sakura Finetek), snap frozen in liquid N₂ and stored at -80°C until use. For the histological assessment of fibrosis, hearts from 3 and 6 months old KO and WT mice ($n = 5-6$ per genotype, sex and age) were stained with Masson's trichrome (Sigma-Aldrich, Procedure No. HT15). Per heart, at least 3 serial transverse sections of 10 µm were examined using a Zeiss Stemi 2000-C microscope.

The cardiomyocytes' cross-sectional area was determined using 3.5 months old female KO and WT mice ($n = 3-4$). Per

section, 4-6 random fields of reticulin membrane staining (Sigma Aldrich, Procedure No. HT102) were digitalized using a bright-field microscope at 40× magnification and cell areas ($n = 1000-1200$) in pixels were calculated with ImageJ version 1.37 software (<http://rsb.info.nih.gov/ij>).

Cardiac catheterization

Heart function was measured in 3.5 months old S100A1KO and WT mice with a C57BL/6J background deriving from homozygous mutant and WT parents, respectively, and in 7 months old littermate mice with a mixed C57BL/6-129/SvEv background with 1.4 French ultraminiature catheter pressure transducers (SPR-671, Millar Instrument Inc.) in closed-chest spontaneously breathing animals anaesthetized with thiopental sodium (Trapanal® 80 mg/kg i.p., Byk Gulden). Briefly, the catheter was placed in the right carotid artery and advanced upstream to the aorta and into the left ventricle (LV). Left-ventricular pressure (P_{\max}) and maximal rates of rise and fall of ventricular pressure (dP/dt_{\max} and dP/dt_{\min}) were continuously recorded. For adrenergic stimulation, a 22 G cannula was placed in the right jugular vein. Dobutamine, isoproterenol and norepinephrine were diluted appropriately in 0.9% NaCl and injected in a 10 µl bolus each by using a precision syringe (Hamilton 702N 25 µl, Hamilton), additionally introducing a spacer so that the tip of the needle was placed at the tip of the cannula in the jugular vein.

Electrocardiogram recordings and analysis

The electrocardiogram (ECG) of S100A1KO and WT littermate mice was recorded and analyzed as previously described (Domenighetti et al. 2007). The following changes were performed: ECG data of each mouse was collected for 5 min under basal conditions, followed by 15 min under isoproterenol stimulation (single, intra-peritoneal injection of 0.15 mg/kg isoproterenol). For each mouse, qualitative analysis of the cardiac rhythm and measurements of the heart rate (HR) was performed on 5 plus 15 min of continuous experimental recording. Quantitative analysis of interval durations was carried out on a 30-s interval taken ~2 min after the beginning of recording and ~2 min after injection. Modified QRS complexes reminiscent of bundle branch block were excluded from interval calculations. Corrected QT intervals (QTc) were calculated according to $QTc = QT/(RR/100)^{1/2}$ (Mitchell et al. 1998).

RNA isolation, reverse transcription (RT), polymerase chain reaction (PCR), quantitative real-time PCR, Affymetrix gene expression profiling and bioinformatics

For expression analysis, heart RNA from S100A1KO and WT littermate mice was used. Total RNA was extracted from liquid N₂-frozen S100A1KO and WT ventricles (RNeasy, Qiagen), tested for purity (A_{260}/A_{280} close to 2.0) and integ-

rity (28S/18S rRNA intensity close to 2 : 1) using an Agilent 2100 bioanalyzer. RT and PCR were performed as described previously (Ackermann et al. 2006).

For quantitative real-time PCR, dilution series of 80, 40, 20 and 10 ng cDNA was combined with TaqMan Universal PCR Master Mix (4304437, Applied Biosystems) and the respective Assays-on-demand mixes (Mm004478585_m1 [S100A1], Mm00485897_m1 [S100B], Mm00803372_g1 [S100A4], Mm00477273_m1 [S100A13], Mm00486655_m1 [calmodulin 1], Mm00437164_m1 [troponin I], Mm00439040_m1 [GABA_A receptor α 1], all from Applied Biosystems) to a total volume of 25 μ l, and submitted to single initial incubation steps at 50°C, 2 min and 95°C, 10 min, followed by 40 cycles of denaturation at 95°C, 15 s, annealing at 60°C, 1 min, and elongation at 60°C, 1 min, in an ABI PRISM 7700 Sequence Detector. Data was recorded and processed using Sequence Detection Software, Version 8.6. Gene expression data was normalized to the expression level of troponin I, and KO values were related to WT according to the formula $2^{-\Delta\Delta CT}$ (User Bulletin #2, Applied Biosystems).

For Affymetrix gene expression profiling, 5 μ g total RNA was used for one-cycle cDNA synthesis (Affymetrix P/N 900432). Double-stranded cDNA was cleaned up (Affymetrix P/N 900371), submitted to biotin-labeled cRNA synthesis (Affymetrix P/N 900449), cleaned up and quantified using an Agilent 2100 bioanalyzer. For hybridization, 15 μ g of the adjusted cRNA yield was fragmented, mixed with hybridization controls, herring sperm DNA, acetylated BSA, hybridization buffer and DMSO, injected into pre-hybridized gene arrays (Mouse 430A Affymetrix P/N 900412) and incubated for 16 h at 45°C. Chips were washed, stained and scanned (Affymetrix GS 3000 scanner) using antibody-based fluorescence signal amplification. Cell intensity data (.cel files) were submitted to scaling and batch analysis (.chp files). Gene expression data was normalized and expressed in fold change using GeneSpring, Version 7.1 (Silicon Genetics).

Protein extraction and immunostainings

S100A1KO and WT male and female littermate mice were anesthetized in their home cages by isoflurane to prevent catecholaminergic fight and flight reactions, which would alter the phosphorylation states of key regulatory proteins in the heart. Subsequently, mice were deeply anesthetized with pentobarbital (160 μ g Nembutal per g body weight) and killed at rest by heart dissection. Hearts were immediately frozen in liquid N₂, pulverized in a liquid N₂-cooled mortar using a pestle and homogenized in 3 ml ice-cold extraction buffer (40 mmol/l Tris-HCl, pH 7.4, 4% CHAPS, Protease Inhibitor Cocktail [Roche] and Phosphatase Inhibitor Cocktail 1 and 2 [Sigma]) by vortexing and ultrasonication (4 × 30 s on ice). The heart protein suspension was centrifuged at 1000 g for 10 min, 4°C, and the pellet was kept on ice for the isolation of nuclear

proteins. The supernatant was centrifuged at 100'000 g for 2 h, 4°C, and the resulting supernatant (cytosol) was kept on ice for protein concentration determination. The pellets (nuclear and membrane fraction) were re-suspended in extraction buffer, replacing CHAPS with 1% SDS, vortexed, sonicated and ultracentrifuged as described above. The three supernatants, containing cytosolic, nuclear and membrane proteins, respectively, were submitted to protein concentration determination (2-D Quant Kit, GE Healthcare Europe). Gel electrophoresis and immunoblotting was performed as previously described (Ackermann et al. 2006). Chemiluminescent signal development was achieved using ECL Western Blotting Detection Reagents (GE Healthcare Europe). Antibodies were purchased and diluted as follows: rabbit anti-human S100A1, 1 : 500 (A5109) DakoCytomation; rabbit anti-human S100A13, 1 : 1'000 (2605) (Ridinger et al. 2000); mouse anti-*E. coli* β -galactosidase, 1 : 1'000 (Z378) Promega; goat anti-human PP2B-A α , 1 : 200 (sc-6123); goat anti-human PP2B-A β , 1 : 200 (sc-6124); rabbit anti-human ERG, 1 : 500 (sc-20130); rabbit anti-human GATA-4, 1 : 400 (sc-9053); rabbit anti-human IGFBP3, 1 : 200 (sc-9028); goat anti-human Kir2.4, 1 : 200 (sc-23633); goat anti-human NFATc4, 1 : 200 (sc-1153); rabbit anti-human phospho-NFATc4 (Ser168/170), 1 : 200 (sc-32630-R); goat anti-human NF κ B p50, 1 : 200 (sc-1190); rabbit anti-human NF κ B p65, 1 : 200 (sc-109); goat anti-human SLIT2, 1 : 200 (sc-26601); goat anti-human SOX-7, 1 : 200 (sc-17333), all from Santa Cruz; rabbit anti-actin, 1 : 5'000 (A2066); mouse anti- β -actin, 1 : 4'000 (A5316); mouse anti-chicken tropomyosin, 1 : 40'000 (T9283), all from Sigma; rabbit anti-human calpain 7, 1 : 500 (3377-100); goat anti-cathepsin S, 1 μ g/ml (3366-100); mouse anti-Hsp70, 1 : 4'000 (3096-100), all from Biovision; rabbit anti-human I κ B- α , 1 : 500 (9242); rabbit anti-human PKA C- α , 1 : 1'000 (4782); rabbit anti-human TLR2, 1 : 500 (2229); rabbit anti-human SGK, 1 : 500 (3272); rabbit anti-human p38 MAP kinase, 1 : 1'000 (9212); rabbit anti-human phospho-p38 MAP kinase (Thr180/Tyr182), 1 : 1'000 (9211); rabbit anti-rat p44/42 MAP kinase, 1 : 1'000 (9102); rabbit anti-human phospho-p44/42 MAP kinase (Thr202/Tyr204), 1 : 1'000 (9101); rabbit anti-human JNK, 1 : 1'000 (9252); rabbit anti-human phospho-JNK (Thr183/Tyr185), 1 : 1'000 (9251); rabbit anti-mouse Akt, 1 : 1'000 (9272); rabbit anti-mouse phospho-Akt (Ser473), 1 : 1'000 (9271), all from Cell Signaling; rabbit anti-EGF, 10 μ g/ml (06-102); rabbit anti-human FOXO3A, 1 : 1'000 (07-702); rabbit anti-mouse Notch 4, 1 : 500 (07-189), mouse anti-bovine calmodulin, 1 : 400 (05-173); mouse anti-bovine phospholamban (PLB), 1 : 1'000 (05-205); rabbit anti-human phospho-PLB (Ser16), 1 : 2'000 (07-052); rabbit anti-human phospho- β 2 adrenergic receptor (Thr384), 1 : 500 (07-629), all from Upstate; mouse anti-rabbit α 2 subunit of L-type Ca²⁺ channel, 1 : 500 (MA3-921); mouse anti-rabbit Na⁺/Ca²⁺ exchanger, 1 : 1'000 (MA1-4672); mouse anti-canine SERCA2a, 1 : 1'000 (MA3-919); rabbit anti-canine calsequestrin, 1 : 3'000 (PA1-913), all from Affinity Bioreagents; mouse anti-Dyrk1A,

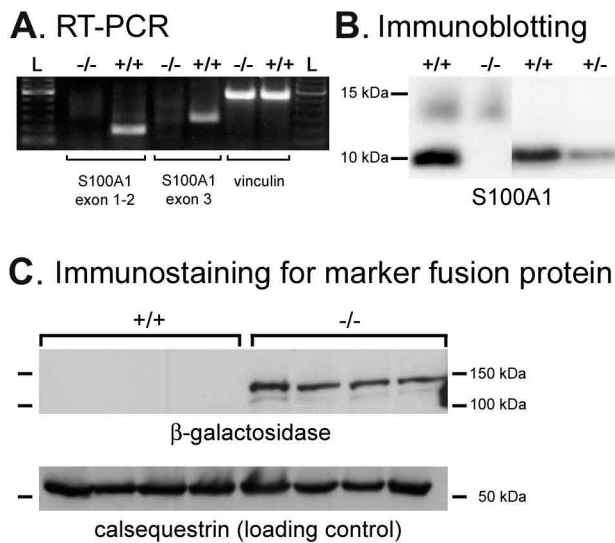


Figure 1. Transcriptional and immunoblot analyses of gene-trapped S100A1 in the heart. **A.** RT-PCR of the 5' and 3' gene trap components using total heart RNA. The 5' component of the gene trap requires transcription from the endogenous S100A1 promoter and includes exons 1 and 2 of S100A1 and the β -galactosidase/neomycin phosphotransferase fusion gene. The 3' component is driven by the phosphoglycerate kinase 1 promoter and includes puromycin *N*-acetyltransferase and exon 3 of S100A1 (Ackermann et al. 2006). S100A1 transcripts of exons 1 and 2 or exon 3 are amplified in WT (+/+) at the expected sizes (191 and 254 bp, respectively), but not in mutant (-/-) hearts. The amplification of vinculin was included in all RT-PCRs as a positive control. L: DNA 100-bp ladder, the brightest band has a size of 600 bp. **B.** Immunoblotting showing the presence of S100A1 in WT (+/+) and heterozygous (+/-), and its absence in mutant (-/-) hearts. **C.** Immunostaining of β -galactosidase and calsequestrin (loading control) by western blotting from protein extracts of WT (+/+) and mutant (-/-) ventricles.

1 : 1'000 (610674); mouse anti-FKBP51, 1 : 500 (610582), both from BD Biosciences; rabbit anti-human PTTG-1, 1 : 1'000 (34-1500) Zymed; rabbit anti-stathmin, 1 : 1'000 (569391) Calbiochem; mouse anti-chicken Na^+/K^+ ATPase, 1 : 500 ($\alpha 6\text{F}$) DSHB; rabbit anti-rat $\text{Ca}_v1.2$ ($\alpha 1\text{c}$ subunit of L-type Ca^{2+} channel) 1 : 800 (ACC-003) Alomone Labs; rabbit anti-phospho-PLB (Thr17), 1 : 4'000 (A010-13) Badrilla Ltd.; rabbit anti-GABA_A receptor $\alpha 1$, 1 : 2'000, was generously provided by J.-M. Fritschy, University of Zürich, Zürich. For immunoblot quantification, band intensities of 3–8 individual mice per genotype and sex were determined by Quantity One (Version 4.6), Biorad, using the local background subtraction mode and Ponceau red total protein stain for normalization.

Statistics

For statistical analysis, *p*-values were calculated by two-way factorial ANOVA with genotype and sex as between-subject

factors (SPSS, Version 11.5). When dobutamine, isoproterenol or norepinephrine was applied, the repeated-measurement model was used with 'dose' as within-subject factors and 'genotype' and 'sex' as between-subject factors. Unpaired *t*-tests were performed when only two groups were compared, i.e. KO versus WT. Effects were considered significant if *p* < 0.05. Mean gene expression levels between ventricular transcriptomes of male and female S100A1KO and WT (*n* = 5 per genotype and sex) were statistically compared using parametric (*t*-test) and non-parametric (Mann-Whitney U test) tests. Differences in gene expression were considered significant if *p* < 0.01, and relevant if fold change was >1.5 or <0.67, respectively.

Results

Mice with a retroviral gene trap insertion in the S100A1 locus do not express S100A1 mRNA or protein

The generation of loss-of-function mutations by gene trapping is an alternative to targeted mutagenesis by homologous recombination in the mouse (Zambrowicz et al. 1998). We have used the former method to disrupt the S100A1 gene with a retroviral insertion between exon 2 and 3 (Ackermann et al. 2006), whereas Du et al. have used the latter to delete the protein coding regions of exon 2 and 3 (Du et al. 2002). As shown previously by northern blot analysis, full-length S100A1 transcripts were absent in gene-trapped mutants in any tissue where S100A1 is normally expressed, including the heart (Ackermann et al. 2006). Likewise, lack of cardiac S100A1 mRNA encompassing exons 1 and 2 or exon 3, respectively, was confirmed by RT-PCR (Fig. 1A). Immunoblot analysis proved the absence of S100A1 in the mutant heart, and ventricles from heterozygous (+/-) mice contained about half the levels of S100A1 when compared to WT (Fig. 1B). The presence of the gene trap marker β -galactosidase demonstrates the functionality of the endogenous S100A1 promoter in the heart of mutant mice (Fig. 1C), and polyclonal anti-S100A1 antibodies did not react with proteins of the size of β -galactosidase in S100A1-deficient (S100A1 knock out, S100A1KO) ventricular extracts (data not shown), which confirms the results from the transcriptional analysis and suggests that the coding region of S100A1 exon 2 is not part of the marker fusion protein.

S100A1KO mice show normal heart sizes and histology

In order to evaluate the effects of S100A1 loss-of-function on heart size and histology, we determined heart and body weights, heart-body weight indices, potential cardiac fibrosis and cardiomyocyte size in S100A1KO and WT mice. Heart weights, body weights as well as heart-body weight ratios were unchanged in S100A1KO mice, and no fibrosis was observed in mutants up to 6 months

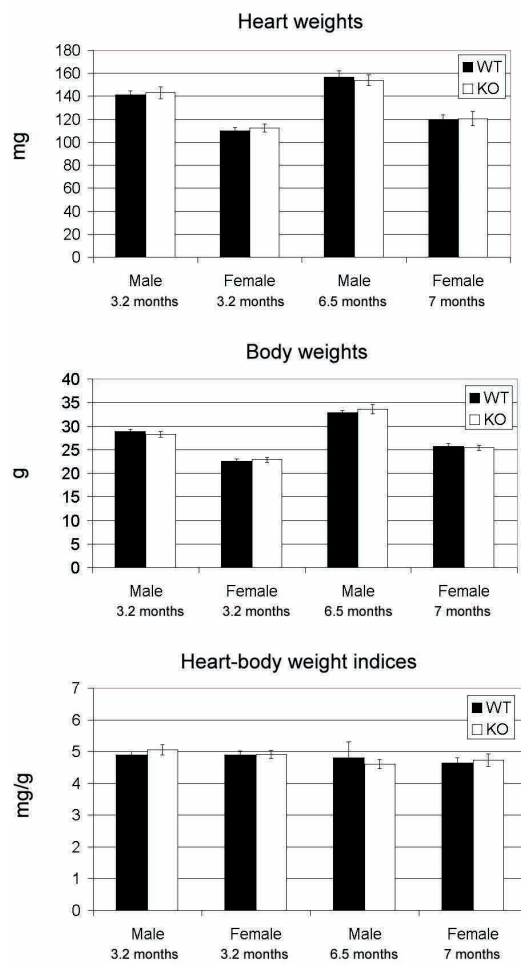
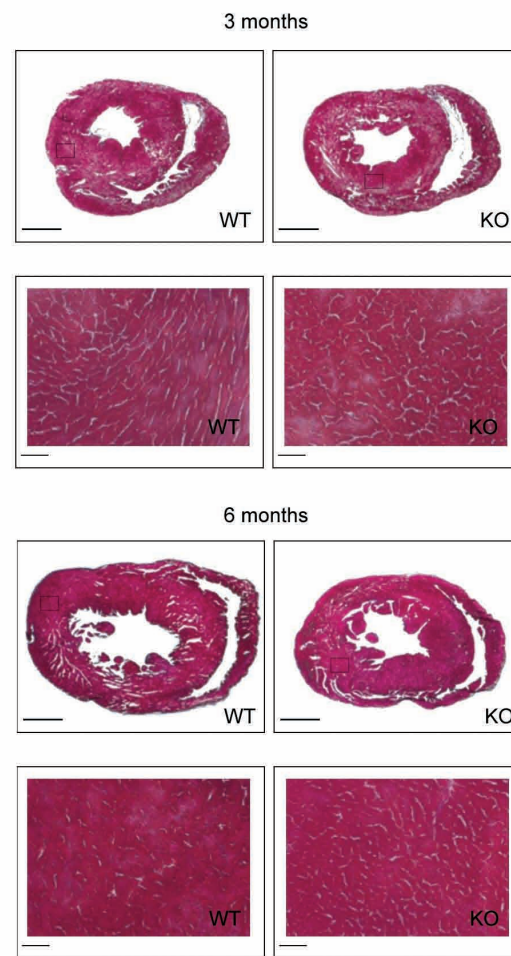
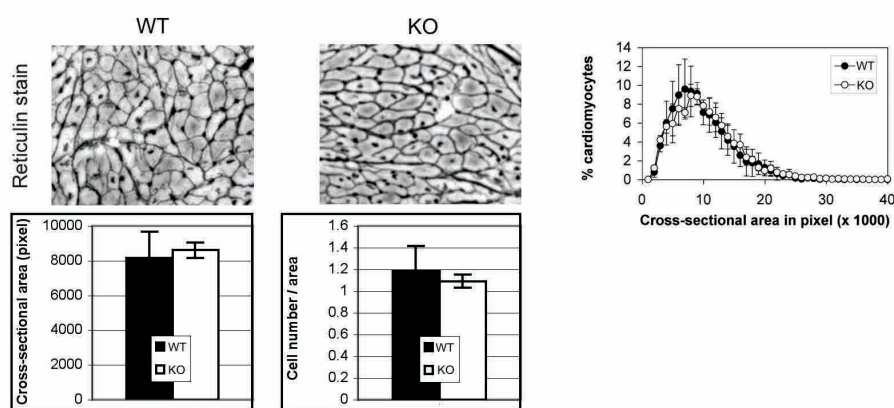
A. Heart and body weights**B. Masson's trichrome staining****C. Cell area and cell size distribution**

Figure 2. Gross cardiac characterization. **A.** Heart and body weights and their ratios (indices) of S100A1KO and WT mice at the mean ages of 3.2 months (15 males and 18 females), 6.5 months (17 males) and 7 months (11 females). Shown are the means \pm SEM. **B.** Masson's trichrome staining of transverse heart sections from 3 and 6 months old S100A1KO and WT mice. Framed regions are shown at higher magnification. Normal cardiac tissue appears in pink, interstitial fibrosis would be visible in blue. Scale bars: whole heart sections, 1 mm; high magnification view, 50 μ m. **C.** Determination of cell area (left) and cell size distribution (right) on transverse heart sections of 3.5 months old S100A1KO and WT mice. Reticulin staining was performed to mark the sarcolemma for cell area measurements using the ImageJ software.

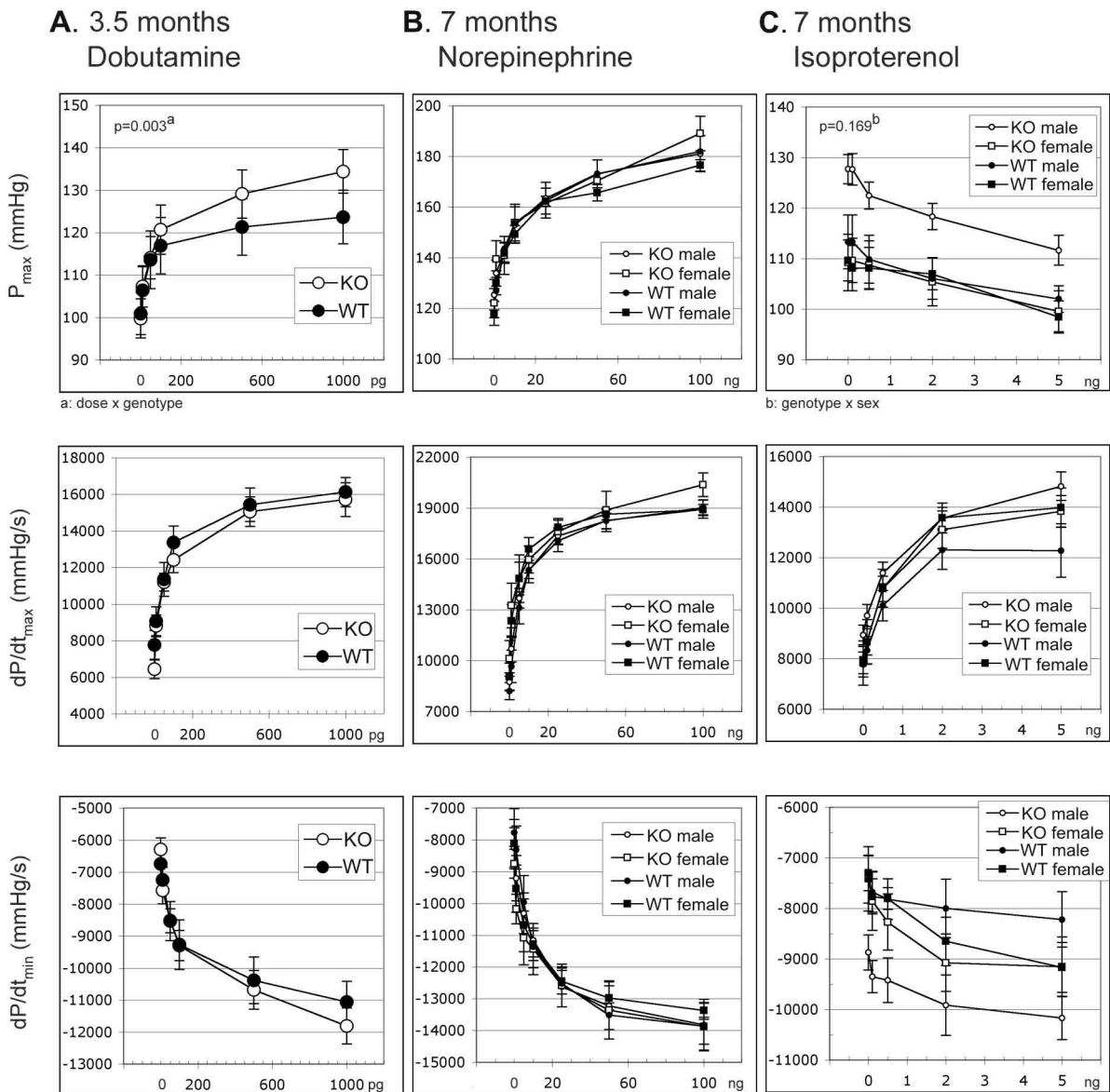


Figure 3. Invasive hemodynamic measurements in S100A1KO and WT mice. Shown are LV systolic pressure (P_{\max}) and maximal rates of rise (dP/dt_{\max}) and fall (dP/dt_{\min}) in LV pressure at rest (dose 0) and after increasing doses of adrenergic stimulation by (A) dobutamine, (B) norepinephrine or (C) isoproterenol. For 3.5 months old mice, $n = 6$ per genotype; for 7 months old mice, $n = 4-7$ per genotype and sex. Data are means \pm SEM.

of age (Fig. 2A,B). In addition, the cross-sectional area of cardiomyocytes and their size distribution as measured on heart sections were similar in 3 months old S100A1KO and WT mice (Fig. 2C).

β_1 -adrenergic stimulation results in systolic pressure elevation in 3.5 months old S100A1KO mice

To evaluate the consequences of S100A1 deficiency on heart function, invasive hemodynamic measurements

were performed. At rest, 3.5 months old KO and WT mice showed similar left-ventricular systolic and diastolic pressures, and resembling contraction (dP/dt_{\max}) and relaxation (dP/dt_{\min}) rates, indicating essentially normal cardiac function in the absence of S100A1 under baseline conditions. Upon stimulation with increasing doses of the β_1 -adrenergic receptor agonist dobutamine, S100A1KO mice responded with a significantly pronounced rise in left-ventricular systolic pressures ($p = 0.003$), whereas contraction and relaxation rates were comparable to those of WT

Table 1. Electrocardiogram parameters of S100A1KO and WT mice by age and isoproterenol treatment (measures are given in mean \pm SD)

		Intervals (ms)													
		PR		QRS		QT		QTc		ST		RR		HR (beats/min)	
		rest	iso	rest	iso	rest	iso	rest	iso	rest	iso	rest	iso	rest	iso
3.5 months	WT ($n = 14$)	47 \pm 5	52 \pm 7	12 \pm 1	12 \pm 1	61 \pm 5	56 \pm 3	51 \pm 4	53 \pm 2	49 \pm 4	44 \pm 3	142 \pm 17	115 \pm 9	429 \pm 56	527 \pm 39
	KO ($n = 17$)	45 \pm 3	50 \pm 6	12 \pm 1	12 \pm 1	61 \pm 5	60 \pm 8	50 \pm 4	56 \pm 6	48 \pm 4	48 \pm 8	148 \pm 11	115 \pm 7	408 \pm 32	524 \pm 32
6.5 months	WT ($n = 15$)	44 \pm 3	46 \pm 4	11 \pm 1	11 \pm 1	55 \pm 4	55 \pm 3	47 \pm 3	52 \pm 3	44 \pm 3	44 \pm 4	136 \pm 13	109 \pm 6	444 \pm 41	551 \pm 30
	KO ($n = 15$)	43 \pm 4	44 \pm 4	12 \pm 1	12 \pm 1	57 \pm 4	61 \pm 6	49 \pm 4	58 \pm 5	45 \pm 4	49 \pm 5	137 \pm 18	109 \pm 6	444 \pm 61	553 \pm 30
12–20 months	WT ($n = 14$)	46 \pm 3	47 \pm 4	12 \pm 1	11 \pm 1	57 \pm 4	57 \pm 4	49 \pm 4	54 \pm 4	46 \pm 4	45 \pm 4	139 \pm 13	112 \pm 5	436 \pm 39	535 \pm 24
	KO ($n = 12$)	45 \pm 3	44 \pm 4	12 \pm 2	12 \pm 1	59 \pm 4	64 \pm 7	50 \pm 4	60 \pm 6	47 \pm 4	51 \pm 7	144 \pm 17	114 \pm 7	421 \pm 50	530 \pm 31

Table 2. Summary of p-values and interaction of ECG parameters of S100A1KO and WT mice by age

		Dependent variable						
			PR	QRS	QT	QTc	ST	RR
3.5 months	t \times g	ns	ns	0.046 \uparrow i	0.006 \uparrow i	0.032 \uparrow i	ns	ns
	t \times g \times s	ns	ns	ns	ns	ns	ns	ns
6.5 months	t \times g	ns	ns	0.045 \uparrow i	0.046 \uparrow i	0.032 \uparrow i	ns	ns
	t \times g \times s	ns	ns	ns	ns	ns	ns	ns
12–20 months	t \times g	0.024 \downarrow i	ns	0.042 \uparrow i	0.019 \uparrow i	0.037 \uparrow i	ns	ns
	t \times g \times s	0.01 \downarrow im	ns	ns	ns	ns	ns	ns

t, treatment; g, genotype; s, sex; ns, not significant; \uparrow i/ \downarrow i, interval significantly increased/decreased in isoproterenol-treated KO; m, significant male-specific difference.

mice (Fig. 3A). There was no significant ‘dose \times genotype \times sex’ interaction, although separate analyses of male and female mice suggested that male mice contributed more to the overall effect.

Since these results are contrary to what has already been published on another mouse line of S100A1 deficiency, we repeated hemodynamic measurements with cohorts of our mouse line that more closely matched the conditions used by Du et al. (2002). Therefore, we used older mice (7 months) of a mixed genetic background (C57BL/6-129/SvEv) and isoproterenol for stimulation. Again, our results did not show impaired contractility and relaxation in response to β -adrenergic stimulation as reported by Du et al. (2002). In contrast, we found normal cardiac function in S100A1KO mice upon norepinephrine and isoproterenol stimulation (Fig. 3B,C). Even though the left-ventricular systolic pressure seems to be increased in 7 months old KO males as a result of a baseline effect, there was no ‘genotype \times sex’ interaction (Fig. 3C). Considering the unchanged cardiac performance at rest and upon norepinephrine stimulation in 7 months old KO mice (Fig. 3B), we conclude that the loss of S100A1 does not impair the inotropic or lusitropic response of the heart.

In response to β -adrenergic signaling, S100A1KO mice display cardiac repolarization and conduction abnormalities

To determine whether the loss of S100A1 is associated with electrical alterations, we examined the electrocardiogram (ECG) of S100A1KO and WT mice at rest and in response to isoproterenol at different ages. ECG interval measurements and statistical analyses are given in Tables 1 and 2, respectively.

The PR interval represents the time the electrical impulse takes to travel along the cardiac conduction system from the beginning of atrial depolarization to the beginning of ventricular depolarization. Whereas no striking genotypic differences were found in younger mice (mean age of 3.5 or 6.5 months), S100A1KO mice aged 12–20 months displayed significantly shortened PR intervals in response to isoproterenol administration when compared to equally treated WT siblings of the same age (Fig. 4A). This effect was contributed by male S100A1KO mice as the ‘treatment \times genotype \times sex’ interaction was significant (Table 2). The PR interval, which represents atrial depolarization, was unchanged in mutant mice (data not shown), implying that shortened PR intervals are due to accelerated AV node conduction.

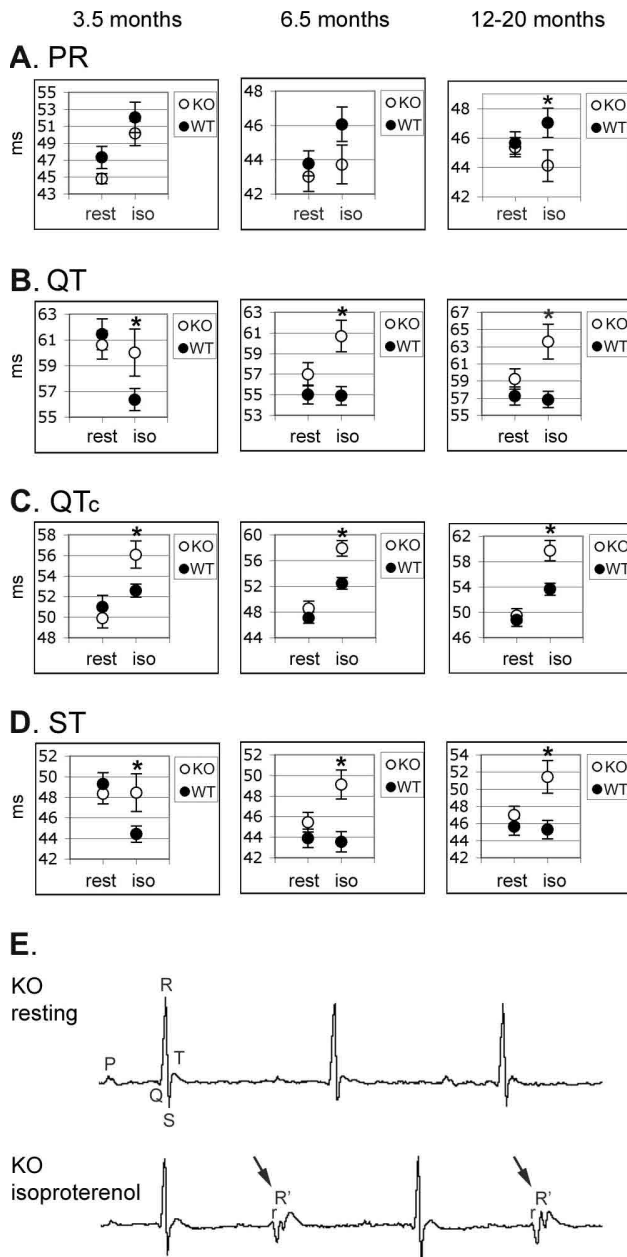


Figure 4. Electrical activity of the heart as determined by ECG recordings. Shown are values in milliseconds (ms; mean \pm SEM; *, $p < 0.05$) of 3.5 months, 6.5 months and 12–20 months old S100A1KO and WT mice at rest and after isoproterenol administration. **A.** PR interval. **B.** QT interval. **C.** Heart rate-corrected QT interval (QTc). **D.** ST interval. **E.** Representative ECG recordings from lead I of KO mice at rest and after β -adrenergic stimulation. Indicated are the waves of normal electrical excitation (PQRST) and of alternating modified depolarization complexes (arrows, r and R' waves) after isoproterenol injection.

While the duration of ventricular depolarization (QRS interval) was similar in KO and WT mice, both, at rest and upon β -adrenergic stimulation, isoproterenol treat-

ment resulted in significantly prolonged QT, QTc and ST intervals in KO mice of all age classes (Fig. 4B–D). These data indicate that upon β -adrenergic stimulation, the time for ventricular repolarization is extended in S100A1KO mice when compared to equally treated age-matched WT, although no differences in heart rate (HR) or cardiac cycle (RR interval) were observed.

The loss of S100A1 was moreover associated with isoproterenol-induced intraventricular conduction disturbances (Fig. 4E). The observed pattern is reminiscent of bundle branch block with 2 : 1 periodicity, displaying alternating normal QRS complexes and complexes with r and R' waves that are likely illustrating intraventricular conduction delay. Such abnormal QRS complexes were not observed in WT mice (data not shown).

In summary, these findings indicate that in response to β -adrenergic signaling loss of S100A1 results in prolonged ventricular repolarization and disturbed intraventricular conduction displaying characteristics of 2 : 1 bundle branch block.

Transcriptional profiling of the S100A1KO ventricular myocardium

To seek a molecular signature for the observed phenotypic alterations conferred by the absence of S100A1, we compared microarray gene expression profiles of the ventricular myocardium from 6 months old S100A1KO and WT mice ($n = 5$ per genotype and sex). Out of approximately 11'000 detectable myocardial transcripts, only 14 genes were consistently up- and down-regulated in both sexes lacking S100A1 (Table 3.1). The majority of the differentially expressed genes (168) was sex-specific, i.e. significantly up- or down-regulated in S100A1-deficient males or females only (Tables 3.2–3.4 and 4).

Strikingly, the most down-regulated genes in the two mutant sexes, besides S100A1, were ion channels, i.e. the inwardly-rectifying K^+ channel *Kcnj14* (Kir2.4) [$\downarrow 5.3\times$] in males and the GABA_A receptor $\alpha 1$ [$\downarrow 8.5\times$] in females (Table 4). Additional differently regulated genes involved in ionic homeostasis in KO males were the Na^+ channel modifier 1 (*Scn11*) [$\downarrow 1.7\times$], which is a splice factor of the Na^+ channel *Scn8a*, the voltage-gated K^+ channel *Kcnh2* (*Erg1*) [$\downarrow 1.7\times$], which underlies long QT syndrome when less active, the solute carrier family 4, member 3 (anion exchanger AE3) [$\downarrow 1.6\times$], which lowers intracellular pH by inward Cl^- and outward HCO_3^- exchange, the serum/glucocorticoid regulated kinase (SGK) [$\uparrow 2.7$], which modulates Na^+ and K^+ channels, and the Cu^{2+} transporting ATPase, a polypeptide [$\uparrow 2.3\times$], which is implicated in neurological degeneration when mutated. In KO females, further differently regulated genes involved in ionic homeostasis were ras-related associated with diabetes (*Rad*) [$\uparrow 1.8\times$], which inhibits the activity of the L-type Ca^{2+} channel (LTCC) by interacting with its β -subu-

Table 3.1. Transcriptional profiles of ventricles from 6 months old S100A1KO versus WT mice ($n = 5$ per genotype and sex; $p < 0.01$; IB, immunoblot for validation)

1. Similarly regulated in males and females					
male S100A1KO heart			female S100A1KO heart		
Fold change	Gene name		Fold change	Gene name	
up-regulated ↑			up-regulated ↑		
2.799	HRAS-like suppressor		4.688	pituitary tumor-transforming 1 (Pttg1) IB	
2.360	pituitary tumor-transforming 1 (Pttg1) IB		4.174	cytoplasmic FMR1 interacting protein 2	
2.344	cytoplasmic FMR1 interacting protein 2		1.920	HRAS-like suppressor	
down-regulated ↓			down-regulated ↓		
0.005	S100 calcium binding protein A1 (S100A1) IB		0.0053	S100 calcium binding protein A1 (S100A1) IB	
0.289	suppression of tumorigenicity 7-like		0.292	forkhead box O3 (Foxo3) IB	
0.468	exotoses (multiple)-like 2		0.353	FK506 binding protein 5 (FKBP51) IB	
0.470	cathepsin S IB		0.402	neural precursor cell expressed, developmentally down-regulated gene 1 (Nedd1)	
0.494	slit homolog 2 (Drosophila) (Slit2) IB		0.489	cathepsin S IB	
0.498	S100 calcium binding protein A13 (S100A13) IB		0.570	exotoses (multiple)-like 2	
0.509	neural precursor cell expressed, developmentally down-regulated gene 1 (Nedd1)		0.584	glyoxalase 1	
0.558	glyoxalase 1		0.587	slit homolog 2 (Drosophila) (Slit2) IB	
0.596	stathmin 1 IB		0.599	stathmin 1 IB	
0.627	FK506 binding protein 5 (FKBP51) IB		0.607	suppression of tumorigenicity 7-like	
0.654	forkhead box O3 (Foxo3) IB		0.629	S100 calcium binding protein A13 (S100A13) IB	

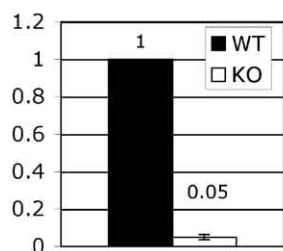
Table 3.2. Transcriptional profiles of ventricles from 6 months old S100A1KO versus WT mice ($n = 5$ per genotype and sex; $p < 0.01$; IB, immunoblot for validation)

2. (Cardiac-specific) transcription, transcriptional activation, myogenesis					
male S100A1KO heart			female S100A1KO heart		
Fold change	Gene name		Fold change	Gene name	
up-regulated ↑			up-regulated ↑		
4.513	Down syndrome critical region homolog 1 (human) (Dscr1)		2.929	nuclear receptor subfamily 4, group A, member 1	
2.249	dual-specificity tyrosine-(Y)-phosphorylation regulated kinase 1a (Dyrk1a) IB		1.861	paired related homeobox 1 (Prx1)	
1.919	Kruppel-like factor 4 (gut)		1.661	Cbp/p300-interacting transactivator, with Glu/Asp-rich carboxy-terminal domain, 4	
down-regulated ↓			down-regulated ↓		
0.596	jumonji, AT rich interactive domain 2		0.292	forkhead box O3 (Foxo3) IB	
0.631	thyrotroph embryonic factor		0.470	nephroblastoma overexpressed gene	
0.642	SRY-box containing gene 7 IB		0.471	nuclear factor I/A	
0.654	forkhead box O3 (Foxo3) IB		0.482	small nuclear RNA activating complex, polypeptide 3	
			0.585	Iroquois related homeobox 3 (Drosophila)	
			0.610	cyclin T2	

Table 3.3. Transcriptional profiles of ventricles from 6 months old S100A1KO versus WT mice ($n = 5$ per genotype and sex; $p < 0.01$)

3. Fatty acid, glucose, carbohydrate metabolism			
male S100A1KO heart		female S100A1KO heart	
Fold change	Gene name	Fold change	Gene name
up-regulated ↑		up-regulated ↑	
1.935	Kruppel-like factor 2 (lung)	1.684	3-hydroxybutyrate dehydrogenase (heart, mitochondrial)
1.517	2,3-bisphosphoglycerate mutase		
1.501	Bernardinelli-Seip congenital lipodystrophy 2 homolog (human)		
down-regulated ↓		down-regulated ↓	
0.628	Coenzyme A synthase	0.529	McKusick-Kaufman syndrome protein
0.650	plasma membrane associated protein, S3-12	0.599	heat shock 70kD protein 5 (glucose-regulated protein)
0.653	fatty acid synthase	0.606	carnitine O-octanoyltransferase
		0.612	6-phosphofructo-2-kinase/fructose-2,6-biphosphatase 1
		0.617	thioredoxin interacting protein

Expression levels of GABA_A receptor α 1 (females, $n=5$, $p<0.0001$)



Expression levels of S100A13 (males, $n=4$, $p<0.0001$)

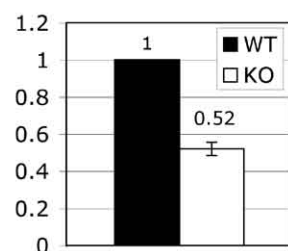


Figure 5. Ventricular expression levels in fold change of GABA_A receptor α 1 and S100A13 transcripts in S100A1KO relative to WT at 6 months of age as estimated by real-time RT-PCR. The expression of troponin I was used for normalization.

nit, the solute carrier family 22/member 3 (organic cation transporter) [$\uparrow 1.8\times$], which is Na⁺-driven and involved in the inactivation of catecholamines, the Na⁺/K⁺ transporting ATPase β 2 polypeptide [$\uparrow 1.5\times$], which has a major role in the membrane recruitment of the Na⁺/K⁺ ATPase, and the voltage-gated Na⁺ channel, type IV, α polypeptide (Scn4a) [$\uparrow 1.5\times$], which can underlay long QT syndrome when Na⁺ current is increased (Table 4).

There were no major gene clusters activated or suppressed by the absence of S100A1. Instead, a more nuanced profile was seen in which genes of several cellular processes and networks were found to be differently controlled. Nevertheless, genes involved in transcriptional activation in general or specifically of the cardiac program, as well as genes of the energy metabolism represented considerable groups responsive to the loss of S100A1 (Tables 3.2 and 3.3). In addition,

genes of the immune and apoptotic/survival response, of oncogenic and tumor suppressive activity, involved in protein cleavage, folding and cytoskeleton remodeling, participating in G-protein and phosphatase signaling, and controlling further cellular processes were also significantly regulated in S100A1KO hearts (Table 3.4).

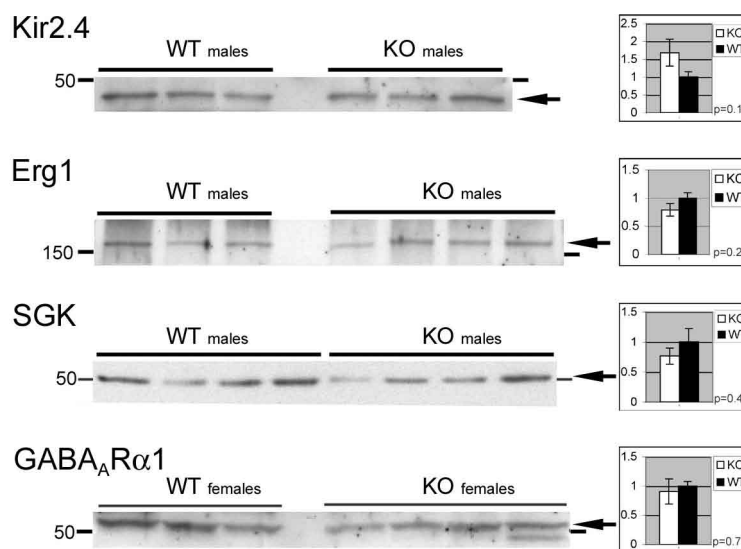
No compensatory up-regulation of S100 protein family members or other structurally related Ca²⁺-binding proteins were found in S100A1-deficient hearts. Instead, S100A13, which lays upstream of the S100A1 locus, was down-regulated in males [$\downarrow 2\times$] and females [$\downarrow 1.6\times$] (Table 3.1). The transcription of the local downstream neighbour of S100A1, 2500003M10Rik, was unchanged. This suggests that the genes neighbouring the S100A1 locus are not severely perturbed by the integrated gene trap vector.

To validate our microarray gene expression data, quantitative real-time RT-PCR was performed on separate specimens for pertinent genes, such as S100A1, GABA_A receptor α 1 as well as S100A13, and expression levels were normalized to troponin I. Results from quantitative real-time RT-PCR and gene array hybridization corresponded well and mutually confirmed their reliability, i.e. real-time RT-PCR revealed a 20 \times down-regulation of GABA_A receptor α 1 mRNA and a 2 \times down-regulation of S100A13 in the KO (Fig. 5). S100A1 transcripts were not detectable in KO ventricles by real-time RT-PCR after 40 amplification cycles (data not shown).

Immunoblot analysis of differentially regulated genes

In order to investigate whether the observed repolarization deficits in S100A1KO mice are associated with limiting

Figure 6. Immunoblot analysis of differentially regulated genes as determined in the gene array survey. Shown are representative western blots of ventricular extracts of S100A1KO and WT mice stained with antibodies against the K⁺ channels Kir2.4 and Erg1, the serum/glucocorticoid-regulated kinase SGK and the Cl⁻ channel subunit GABA_A receptor α 1. Kir2.4 and GABA_A receptor α 1 were the most prominently down-regulated genes in the gene array survey in KO males [\downarrow 5.29] and KO females [\downarrow 8.47], respectively. Additionally, Erg1 was down-regulated by a factor of \downarrow 1.69 and SGK up-regulated by a factor of \uparrow 2.3 in KO males. Arrows indicate specific protein bands, numbers molecular weight in kDa. Plots represent band intensities of the respective protein normalized to Ponceau red (means \pm SEM).



amounts of the potassium channels Kir2.4 [\downarrow 5.3 \times] and Erg1 [\downarrow 1.7 \times] in KO males, and the chloride channel subunit GABA_A receptor α 1 [\downarrow 8.5 \times] in KO females, we analyzed ventricular extracts of 6 months old KO and WT mice by immunoblotting and verified our results on additional specimens from older mice. Surprisingly, none of the gene array candidates involved in ion flux regulation was significantly up- or down-regulated in the KO proteom (Fig. 6). We further probed all differentially regulated genes of which antibodies were available to us (Tables 3.1–3.4, indicated by IB) and again did not find significant changes in KO versus WT by immunoblotting (data not shown).

Since several of the differentially regulated genes are part of signaling pathways that lead to the activation of key transcription factors, we have checked level and phosphorylation states of Akt, p42/44 and p38 Map kinases, Jun-N-terminal kinase (JNK) and nuclear factor of activated T cells (NFATc4), as well as level and intracellular localization of GATA-4, NF κ B p50 and p65. Once more, we did not see significant differences between KO and WT by immunoblotting (data not shown).

As S100A1 is considered a Ca²⁺-dependent regulator of excitation-contraction coupling (reviewed in Most et al. 2007), we have additionally determined the level of proteins involved in Ca²⁺ handling, such as the LTCC, Na⁺/Ca²⁺ exchanger, SERCA2a, calsequestrin, calmodulin and PLB. Since the activity of PLB is modulated by protein kinase A (PKA) and Ca²⁺/calmodulin-dependent kinase II (CaMKII) in a Ca²⁺-dependent manner, we have determined the phosphorylation state of PLB at Ser16 (PKA) and Thr17 (CaMKII) by immunoblotting (Fig. 7). Again, we did not observe significant differences between S100A1KO and WT mice, neither regarding protein levels nor phosphorylation extents.

Taken together, we conclude that loss of S100A1 significantly affects transcription as determined by the microarray gene expression survey; the protein inventory, however, was found to be less susceptible for changes and not significantly impacted by S100A1 deficiency.

Discussion

S100A1 was initially identified as a regulator of cardiac contractile performance. It was shown to enhance intracellular Ca²⁺ cycling by interacting with SERCA2a, PLB and the RyR2, resulting in increased SR Ca²⁺ reuptake and excitation-contraction coupling gain (reviewed in Donato 2003; Zimmer et al. 2003; Most et al. 2007). A novel function of S100A1 has recently been considered as S100A1 was shown to interact with and regulate the F1 subunit of the ATP synthase (Boerries et al. 2007). Here we report that loss of S100A1 is associated with catecholamine-induced prolonged QT, QTc and ST intervals and the propensity for ventricular conduction disturbances. In addition, we identified genes by transcriptome profiling that were differentially regulated in the S100A1-deficient myocardium, providing a molecular signature for the observed phenotypic alterations. Taking into account that studying the role of S100A1 in a mouse knock out model does not unambiguously allow dissecting causative and compensatory effects of S100A1 loss of function, our data shows that S100A1 contributes to the electrical homeostasis of the heart.

Whereas a previously published mouse model of S100A1 deficiency generated by exon deletion was characterized by impaired inotropic and lusitropic responses upon β -adrenergic stimulation (Du et al. 2002), our mouse model generated

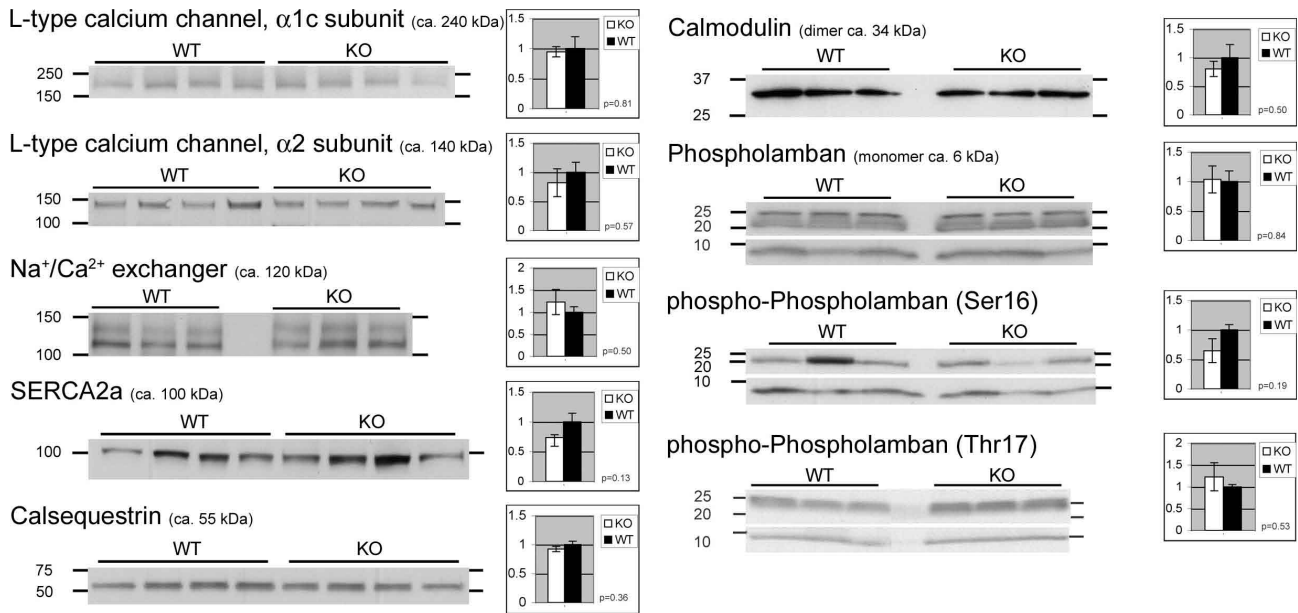


Figure 7. Levels of Ca^{2+} -transporting and -binding proteins including phosphorylation state of PLB in S100A1KO and WT ventricular extracts. Shown are representative immunoblots of the L-type Ca^{2+} channel $\alpha 1c$ and $\alpha 2$ subunits, $\text{Na}^+/\text{Ca}^{2+}$ exchanger, SERCA2a, calsequestrin, calmodulin, PLB and phosphorylated PLB at Ser16 and Thr17. Numbers indicate molecular weight in kDa. Plots represent band intensities of the respective protein normalized to Ponceau red (means \pm SEM).

by gene trap mutagenesis does not show these phenotypic characteristics. In contrast, our S100A1KO mice showed normal or even enhanced cardiac contraction (Fig. 3), i.e. 3.5 months old S100A1KO mice presented with significantly augmented left-ventricular systolic pressures upon application of increasing doses of dobutamine.

Although the genetic background of the two S100A1-deficient mouse lines is similar, the epigenetic consequences of an exon deletion versus a retroviral insertion may be significant. We therefore checked the expression levels of the genes flanking the S100A1 locus and found S100A13 moderately down-regulated ($\downarrow 2\times$ in KO males and $\downarrow 1.6\times$ in KO females, Table 3.1) and 2500003M10Rik unaffected (data not shown), suggesting that positional effects may not explain the lack of impaired contractility or relaxation in our mouse S100A1KO model.

Prolonged repolarization is manifested in extended QT intervals, which is the defining feature for long QT syndromes (LQTS). Most cases of LQTS derive from either insufficient K^+ efflux or excessive Na^+ or Ca^{2+} influx (including Ca^{2+} ions released from the SR) during the ventricular action potential (Roepke and Abbott 2006). These ionic imbalances delay myocardial repolarization, which can result in unwanted depolarizations (early and late after-depolarizations), possibly leading to ‘torsades de pointes’, ventricular tachycardia, ventricular fibrillation, syncope and sudden cardiac death. Independent of whether LQTS are inherited or acquired, the

primary mechanism of arrhythmia susceptibility points to ion channels that are affected by mutations, altered interacting proteins, posttranslational modifications or metabolic changes (Keating and Sanguinetti 2001; Wilde and Bezzina 2005). The occurrence of prolonged QT, QTc and ST intervals upon β -adrenergic signaling in S100A1-deficient mice indicates that S100A1 can be considered as a candidate underlying LQTS of so far unknown etiology.

The bundle branch block with 2 : 1 periodicity as manifested in a pattern of normal and modified QRS complexes in isoproterenol-stimulated KO mice may stem from prolonged refractory period in the ventricular conduction pathway in these animals. However, the mechanism underlying this phenomenon is not known and merits to be investigated in a future study.

In summary our results suggest that S100A1 is involved in the spreading of the electrical signal during cardiac de- and repolarization and prevents repolarization delay and bundle branch block under catecholamine-induced stress conditions.

We have done transcriptional profiling to identify changes in cardiac gene expression occurring in the absence of S100A1 that could underlie or compensate for the observed electrical impulse alterations. Indeed, the down-regulation of the K^+ channels Kir2.4 and Erg1 in KO males would be predicted to prolong cardiac repolarization (Table 4). Alternatively, Dscr1, Dyrk1a and calcineurin (PP2B-Aa/ β)

Table 3.4. Transcriptional profiles of ventricles from 6 months old S100A1KO versus WT mice ($n = 5$ per genotype and sex; $p < 0.01$; IB, immunoblot for validation)

4. Others			
male S100A1KO heart		female S100A1KO heart	
Fold change	Gene name	Fold change	Gene name
up-regulated ↑		up-regulated ↑	
5.284	serine (or cysteine) proteinase inhibitor, clade A, member 3N	2.885	immunoglobulin heavy chain 1a (serum IgG2a)
3.342	heat shock protein 1A (Hsp70) IB	2.06	Ras association (RalGDS/AF-6) domain family 2
3.17	ATP-binding cassette, sub-family B (MDR/TAP), member 10	2.025	wingless-related MMTV integration site 5A (Wnt-5a)
3.08	developmental pluripotency-associated 3	2.001	proline-serine-threonine phosphatase-interacting protein 2
2.748	olfactory receptor 56	1.957	E26 avian leukemia oncogene 1, 5' domain
2.691	aminolevulinic acid synthase 2, erythroid	1.945	regulator of nonsense transcripts 1
2.689	sterol-C4-methyl oxidase-like	1.919	ATP-binding cassette, sub-family A (ABC1), member 4
2.55	interleukin 2 receptor, gamma chain	1.916	tropomyosin 2, beta IB
2.314	titin immunoglobulin domain protein (myotilin)	1.895	zinc finger protein 37
2.178	CLIP associating protein 2	1.86	protein tyrosine phosphatase 4a2
2.117	calpain 7 IB	1.752	a disintegrin and metalloproteinase domain 19 (meltrin β)
2.088	microphthalmia-associated transcription factor	1.685	histocompatibility 2, Q region locus 1
1.978	neural precursor cell expressed, developmentally down-regulated gene 9 (Nedd9)	1.664	B-cell CLL/lymphoma 6, member B
1.942	DNA-damage-inducible transcript 4	1.654	epidermal growth factor (EGF) IB
1.903	histocompatibility 2, D region locus 1	1.638	topoisomerase I binding, arginine/serine-rich
1.861	serine/threonine kinase 17b (apoptosis-inducing)	1.628	SWI/SNF related, matrix associated, actin dependent regulator of chromatin, subfamily a, member 4
1.79	a disintegrin-like and metalloprotease (reprolysin type) with thrombospondin type 1 motif, 1	1.612	actin, beta, cytoplasmic IB
1.77	ornithine decarboxylase antizyme inhibitor	1.605	vascular endothelial growth factor A (VEGF A)
1.762	beta-2 microglobulin	1.603	MARCKS-like protein
1.751	Fc receptor, IgG, low affinity IIb	1.573	glutamate-cysteine ligase, modifier subunit
1.749	platelet-derived growth factor, C polypeptide	1.562	mitochondrial ribosomal protein L55
1.747	membrane-spanning 4-domains, subfamily A, member 6C	1.561	eukaryotic translation initiation factor 5
1.729	histocompatibility 2, D region locus 1	1.546	transformation related protein 53
1.714	tubulin, beta 5 IB	1.528	toll-like receptor 2 (Tlr2) IB
1.711	queuine tRNA-ribosyltransferase 1	1.516	CXXC finger 5
1.686	EF hand domain containing 2	1.504	complement component 1, q subcomponent, receptor 1
1.676	ubiquitously transcribed tetratricopeptide repeat gene, X chromosome		
1.649	Casitas B-lineage lymphoma		
1.646	myelin and lymphocyte protein, T-cell differentiation protein		
1.632	ubiquitin specific protease 18		
1.617	dual specificity phosphatase 6		
1.612	receptor (TNFRSF)-interacting serine-threonine kinase 1		
1.606	nucleolar protein 5		
1.598	nuclear factor of kappa light chain gene enhancer in B-cells inhibitor, alpha (I κ B α) IB		
1.578	B-cell translocation gene 2, anti-proliferative		
1.575	neuroblastoma ras oncogene		
1.563	integrin beta 2		
1.551	cyclin L2		
1.539	sortilin-related receptor, LDLR class A repeats-containing		
1.534	ras homolog gene family, member G		
1.511	ATP-binding cassette, sub-family B (MDR/TAP), member 10		
1.506	DnaJ (Hsp40) homolog, subfamily C, member 3		

Table 3.4. (continued)

4. Others			
male S100A1KO heart		female S100A1KO heart	
Fold change	Gene name	Fold change	Gene name
down-regulated ↓		down-regulated ↓	
0.256	ADP-ribosyltransferase (NAD ⁺ ; poly (ADP-ribose polymerase)-like 3	0.294	regulator of G protein signaling 7
0.328	synaptosomal-associated protein 91	0.398	angiopoietin-like 4
0.356	leucine, glutamic acid, lysine family 1 protein	0.476	cancer related gene-liver 1
0.443	chemokine-like factor super family 8	0.477	N-myc downstream regulated 4
0.466	stanniocalcin 2	0.518	insulin-like growth factor binding protein 3 (IGFBP3) IB
0.47	branched chain aminotransferase 2, mitochondrial	0.523	ADP-ribosylation factor 5
0.483	desmocollin 3	0.534	kinesin family member 5B
0.490	6-pyruvoyl-tetrahydropterin synthase	0.547	mitochondrial ribosomal protein L9
0.536	HS1 binding protein 3	0.549	methylocrotonoyl-Coenzyme A carboxylase 1 (alpha)
0.554	cold inducible RNA binding protein	0.556	Yamaguchi sarcoma viral (v-yes) oncogene homolog
0.566	thiosulfate sulfurtransferase, mitochondrial	0.561	phosphodiesterase 7A
0.566	brix domain containing 1	0.564	aminolevulinatase, delta-, dehydratase
0.578	PDZ and LIM domain 7	0.574	pleiomorphic adenoma gene-like 1
0.583	neurturin	0.577	fetal liver zinc finger 1
0.612	protein phosphatase 2, regulatory subunit B (B56), delta isoform (PP2A-Bδ)	0.586	mitochondrial ribosomal protein L9
0.629	ephrin B3	0.587	small nuclear RNA activating complex, polypeptide 3
0.632	protein tyrosine phosphatase 4a3	0.591	B-cell CLL/lymphoma 9
0.64	autophagy 5-like (<i>S. cerevisiae</i>)	0.595	estrogen-related receptor beta like 1
0.644	desmoglein 2	0.605	Notch gene homolog 4 (<i>Drosophila</i>) (Notch4) IB
0.644	ephrin A1	0.609	flavin containing monooxygenase 2
0.647	matrix metalloproteinase 15	0.609	xanthine dehydrogenase
0.648	thyroid hormone receptor interactor 10	0.617	extra cellular link domain-containing 1
0.648	protein kinase, cAMP dependent, catalytic, alpha (PKA C-α) IB	0.618	nucleosome assembly protein 1-like 1
0.65	MAD homolog 7 (<i>Drosophila</i>)	0.618	crumbs homolog 1 (<i>Drosophila</i>)
0.651	tissue factor pathway inhibitor	0.619	nudix (nucleoside diphosphate linked moiety X)-type motif 6
0.654	homocysteine-inducible, endoplasmic reticulum stress-inducible, ubiquitin-like domain member 1	0.625	ethanolamine kinase 1
0.657	CDC-like kinase 3	0.625	phosphodiesterase 7A
0.657	retroviral integration site 2	0.633	syntaxin 18
0.661	CASP2 and RIPK1 domain containing adaptor with death domain	0.635	tumor rejection antigen gp96
0.662	synaptojanin 2	0.638	homocysteine-inducible, endoplasmic reticulum stress-inducible, ubiquitin-like domain member 1
		0.641	CDC-like kinase
		0.642	mitogen-activated protein kinase kinase kinase 6
		0.642	ATPase, H ⁺ transporting, V1 subunit G isoform 1
		0.647	AT rich interactive domain 4B (Rbp1 like)
		0.649	catechol-O-methyltransferase
		0.649	nuclear cap binding protein subunit 2
		0.65	tissue inhibitor of metalloproteinase 4
		0.651	conserved helix-loop-helix ubiquitous kinase
		0.653	phosphomannomutase 1
		0.654	apoptosis-associated speck-like protein containing a CARD
0.655	CDK5 regulatory subunit associated protein 1		
0.663	heterogeneous nuclear ribonucleoprotein C		

Table 4. Transcriptional profiles of ventricles from 6 months old S100A1KO versus WT mice ($n = 5$ per genotype and sex; $p < 0.01$; IB, immunoblot for validation)

Ion channels and related					
male S100A1KO heart			female S100A1KO heart		
Fold change	Gene name		Fold change	Gene name	
up-regulated ↑			up-regulated ↑		
2.713	serum/glucocorticoid regulated kinase (SGK)	IB	1.843	Ras-related associated with diabetes (Rad)	
2.327	ATPase, Cu ²⁺ transporting, alpha polypeptide		1.763	solute carrier family 22 (organic cation transporter), member 3	
			1.519	ATPase, Na ⁺ /K ⁺ transporting, beta 2 polypeptide	IB
			1.514	Na ⁺ channel, voltage-gated, type IV, alpha polypeptide (Scn4a)	
down-regulated ↓			down-regulated ↓		
0.189	potassium inwardly-rectifying channel, subfamily J, member 14 (Kir2.4, voltage gated)	IB	0.118	GABA _A receptor α1	IB
0.581	sodium channel modifier 1 (Scnm1)				
0.591	potassium voltage-gated channel, subfamily H (eag-related), member 2 (Erg1)	IB			
0.613	solute carrier family 4 (anion exchanger), member 3 (AE3)				

act in a common pathway and their respective up- and down-regulation would be assumed to counter excessive Ca²⁺ signaling (Table 3.2) (Arron et al. 2006). Likewise in KO females, up-regulation of the Na⁺/K⁺ ATPase and the Rad GTPase, which has been reported to inhibit LTCC (Yada et al. 2007), would remedy a strained ion homeostasis (Table 4). However, comprehensive immunoblotting revealed that none of the candidate genes for which antibodies were available to us (indicated by IB in Tables 3.1–3.4 and 4) was significantly altered at protein level. With the continuously improving availability of antibodies, it remains to be determined whether other differentially regulated candidate genes may underpin the observed phenotype.

Loss of S100A1, however, impacts on transcription, and further studies may identify transcriptional activators and repressors that regulate gene expression in the state of S100A1 deficiency.

At present, it is not immediately apparent why deletion of the S100A1 gene in mice results in β-adrenergic signaling-triggered prolonged QT, QTc, ST intervals and intraventricular conduction disturbances reminiscent of 2 : 1 bundle branch block. Future studies are needed to clarify the role of S100A1 in the electrical homeostasis of the heart, specifically during ventricular repolarization and in the cardiac conduction system. We speculate that changes in ion fluxes, enzyme activities, protein interaction, localization and/or post-translational modifications account for the observed electrical abnormalities caused by the in vivo loss of S100A1.

In addition, compensatory proteins that function in the state of S100A1 deficiency need to be identified to explain the electrical remodeling provoked by the chronic absence of S100A1 in the heart.

Acknowledgments. The authors thank Claudio Gemperle, Corinne Bosshart and Petra Murmann for excellent technical assistance as well as Prof. Dr. Hugues Abriel, Prof. Dr. Jean-Claude and Evelyne Perriard for invaluable advice.

Sources of Funding. This study was supported by the Swiss National Science Foundation (SNF, grant 3100AO-101970 to C. W. H.), the ‘Stiftung für Herz- und Kreislaufkrankheiten’ (SHK, to P. E.), the Swiss Cardiovascular Research and Training Network (SCRNTN), the Roche Research Foundation, the ‘Novartis Stiftung für Medizinisch-Biologische Forschung’ and the ‘Stiftung für wissenschaftliche Forschung der Universität Zürich’.

References

- Ackermann G. E., Marenholz I., Wolfer D. P., Chan W. Y., Schafer B., Erne P., Heizmann C. W. (2006): S100A1-deficient male mice exhibit increased exploratory activity and reduced anxiety-related responses. *Biochim. Biophys. Acta* **1763**, 1307–1319
- Arron J. R., Winslow M. M., Polleri A., Chang C. P., Wu H., Gao X., Neilson J. R., Chen L., Heit J. J., Kim S. K., Yamasaki N., Miyakawa T., Francke U., Graef I. A., Crabtree G. R. (2006): NFAT dysregulation by increased dosage of DSCR1 and DYRK1A on chromosome 21. *Nature* **441**, 595–600

- Boerries M., Most P., Gledhill J. R., Walker J. E., Katus H. A., Koch W. J., Aebi U., Schoenenberger C. A. (2007): Ca^{2+} -dependent interaction of S100A1 with F1-ATPase leads to an increased ATP content in cardiomyocytes. *Mol. Cell Biol.* **27**, 4365–4373
- Carafoli E. (2003): The calcium-signalling saga: tap water and protein crystals. *Nat. Rev. Mol. Cell Biol.* **4**, 326–332
- Domenighetti A. A., Boixel C., Cefai D., Abriel H., Pedrazzini T. (2007): Chronic angiotensin II stimulation in the heart produces an acquired long QT syndrome associated with IK1 potassium current downregulation. *J. Mol. Cell. Cardiol.* **42**, 63–70
- Donato R. (2003): Intracellular and extracellular roles of S100 proteins. *Microsc. Res. Tech.* **60**, 540–551
- Du X. J., Cole T. J., Tennis N., Gao X. M., Kontgen F., Kemp B. E., Heierhorst J. (2002): Impaired cardiac contractility response to hemodynamic stress in S100A1-deficient mice. *Mol. Cell Biol.* **22**, 2821–2829
- Heizmann C. W., Ackermann G. E., Galichet A. (2007): Pathologies involving the S100 proteins and RAGE. *Subcell. Biochem.* **45**, 93–138
- Keating M. T., Sanguinetti M. C. (2001): Molecular and cellular mechanisms of cardiac arrhythmias. *Cell* **104**, 569–580
- Kiewitz R., Lyons G. E., Schäfer B. W., Heizmann C. W. (2000): Transcriptional regulation of S100A1 and expression during mouse heart development. *Biochim. Biophys. Acta* **1498**, 207–219
- Kiewitz R., Acklin C., Schäfer B. W., Maco B., Uhrík B., Wuytack F., Erne P., Heizmann C. W. (2003): Ca^{2+} -dependent interaction of S100A1 with the sarcoplasmic reticulum Ca^{2+} -ATPase2a and phospholamban in the human heart. *Biochem. Biophys. Res. Commun.* **306**, 550–557
- Marenholz I., Heizmann C. W., Fritz G. (2004): S100 proteins in mouse and man: from evolution to function and pathology (including an update of the nomenclature). *Biochem. Biophys. Res. Commun.* **322**, 1111–1122
- Mitchell G. F., Jeron A., Koren G. (1998): Measurement of heart rate and Q-T interval in the conscious mouse. *Am. J. Physiol.* **274**, H747–751
- Most P., Remppis A., Pleger S. T., Löffler E., Ehlermann P., Bernotat J., Kleuss C., Heierhorst J., Ruiz P., Witt H., Karczewski P., Mao L., Rockman H. A., Duncan S. J., Katus H. A., Koch W. J. (2003): Transgenic overexpression of the Ca^{2+} -binding protein S100A1 in the heart leads to increased in vivo myocardial contractile performance. *J. Biol. Chem.* **278**, 33809–33817
- Most P., Pleger S. T., Völkers M., Heidt B., Boerries M., Weichenhan D., Löffler E., Janssen P. M. L., Eckhart A. D., Martini J., Williams M. L., Katus H. A., Remppis A., Koch W. J. (2004): Cardiac adenoviral S100A1 gene delivery rescues failing myocardium. *J. Clin. Invest.* **114**, 1550–1563
- Most P., Seifert H., Gao E., Funakoshi H., Volkers M., Heierhorst J., Remppis A., Pleger S. T., DeGeorge B. R. Jr., Eckhart A. D., Feldman A. M., Koch W. J. (2006): Cardiac S100A1 protein levels determine contractile performance and propensity toward heart failure after myocardial infarction. *Circulation* **114**, 1258–1268
- Most P., Remppis A., Pleger S. T., Katus H. A., Koch W. J. (2007): S100A1: a novel inotropic regulator of cardiac performance. Transition from molecular physiology to pathophysiological relevance. *Am. J. Physiol.* **293**, R568–577
- Pleger S. T., Most P., Boucher M., Soltys S., Chuprun J. K., Pleger W., Gao E., Dasgupta A., Rengo G., Remppis A., Katus H. A., Eckhart A. D., Rabinowitz J. E., Koch W. J. (2007): Stable myocardial-specific AAV6-S100A1 gene therapy results in chronic functional heart failure rescue. *Circulation* **115**, 2506–2515
- Ridinger K., Schäfer B. W., Durussel I., Cox J. A., Heizmann C. W. (2000): S100A13. Biochemical characterization and subcellular localization in different cell lines. *J. Biol. Chem.* **275**, 8686–8694
- Roepeke T. K., Abbott G. W. (2006): Pharmacogenetics and cardiac ion channels. *Vascul. Pharmacol.* **44**, 90–106
- Santamaria-Kisiel L., Rintala-Dempsey A. C., Shaw G. S. (2006): Calcium-dependent and -independent interactions of the S100 protein family. *Biochem. J.* **396**, 201–214
- Schaub M. C., Heizmann C. W. (2008): Calcium, troponin, calmodulin, S100 proteins: From myocardial basics to new therapeutic strategies. *Biochem. Biophys. Res. Commun.* **369**, 247–264
- Wilde A. A., Bezzina C. R. (2005): Genetics of cardiac arrhythmias. *Heart* **91**, 1352–1358
- Yada H., Murata M., Shimoda K., Yuasa S., Kawaguchi H., Ieda M., Adachi T., Ogawa S., Fukuda K. (2007): Dominant negative suppression of Rad leads to QT prolongation and causes ventricular arrhythmias via modulation of L-type Ca^{2+} channels in the heart. *Circ. Res.* **101**, 69–77
- Zambrowicz B. P., Friedrich G. A., Buxton E. C., Lilleberg S. L., Person C., Sands A. T. (1998): Disruption and sequence identification of 2,000 genes in mouse embryonic stem cells. *Nature* **392**, 608–611
- Zimmer D. B., Wright Sadosky P., Weber D. J. (2003): Molecular mechanisms of S100-target protein interactions. *Microsc. Res. Tech.* **60**, 552–559
- Zimmer D. B., Chaplin J., Baldwin A., Rast M. (2005): S100-mediated signal transduction in the nervous system and neurological diseases. *Cell. Mol. Biol. (Noisy-le-grand)* **51**, 201–214